OncoTargets and Therapy

Dovepress
open access to scientific and medical research

Open Access Full Text Article

CASE REPORT

Molecular diagnostics of a single drug-resistant multiple myeloma case using targeted next-generation sequencing

This article was published in the following Dove Press journal:
OncoTargets and Therapy
5 October 2015
Number of times this article has been viewed

Hiroshi Ikeda[1]
Kazuya Ishiguro[1]
Tetsuyuki Igarashi[1]
Yuka Aoki[1]
Toshiaki Hayashi[1]
Tadao Ishida[1]
Yasushi Sasaki[1,2]
Takashi Tokino[2]
Yasuhisa Shinomura[1]

[1]Department of Gastroenterology, Rheumatology and Clinical Immunology, [2]Medical Genome Sciences, Research Institute for Frontier Medicine, Sapporo Medical University, Sapporo, Japan

Abstract: A 69-year-old man was diagnosed with IgG λ-type multiple myeloma (MM), Stage II in October 2010. He was treated with one cycle of high-dose dexamethasone. After three cycles of bortezomib, the patient exhibited slow elevations in the free light-chain levels and developed a significant new increase of serum M protein. Bone marrow cytogenetic analysis revealed a complex karyotype characteristic of malignant plasma cells. To better understand the molecular pathogenesis of this patient, we sequenced for mutations in the entire coding regions of 409 cancer-related genes using a semiconductor-based sequencing platform. Sequencing analysis revealed eight nonsynonymous somatic mutations in addition to several copy number variants, including CCND1 and RB1. These alterations may play roles in the pathobiology of this disease. This targeted next-generation sequencing can allow for the prediction of drug resistance and facilitate improvements in the treatment of MM patients.

Keywords: multiple myeloma, drug resistance, genome-wide sequencing, semiconductor sequencer, target therapy

Introduction

Multiple myeloma (MM) is characterized by malignant plasma cell proliferation in the bone marrow (BM) associated with monoclonal protein in the serum and/or urine.[1,2] Hematopoietic stem cell transplantation and novel agents such as bortezomib, thalidomide, and lenalidomide have improved the survival of MM patients.[3,4] However, most patients eventually relapse even after the achievement of a complete therapeutic response. Improvements in molecular profiling technologies have provided new insight into the basic molecular events underlying the development of MM as well as the mechanisms of anticancer drug resistance. The transition from the long-established one-size-fits-all approach to new strategies based on individual genetic profiles provides an opportunity to transform current diagnostics into individual prognostic and even predictive classifications.

In MM, there are two distinct genetic subtypes based on copy number alterations and translocations. Approximately half of all MM cases are hyperdiploid, which is characterized by multiple trisomies of chromosomes 3, 5, 7, 9 11, 15, 19, and 21 and a lower prevalence of primary translocations involving the immunoglobulin heavy chain (IgH) locus at 14q32.[5,6] The remaining cases form the nonhyperdiploid group, and chromosomes 8, 13, 14, and 16 are frequently lost. Nonhyperdiploid myeloma is strongly associated with translocations of IgH alleles with various partner chromosomes. Copy number alterations in chromosomal regions, such as 1q, 6q, 8p, and 16q, occur in both subtypes. Overall, nonhyperdiploid MM is associated with worse survival compared with hyperdiploid MM.

Correspondence: Hiroshi Ikeda; Yasushi Sasaki
Department of Gastroenterology, Rheumatology and Clinical Immunology, Medical Genome Sciences, Research Institute for Frontier Medicine, Sapporo Medical University, S-1, W-16, Chuo-ku, Sapporo 060 8543, Japan
Email hiikeda@sapmed.ac.jp; yasushi@sapmed.ac.jp

submit your manuscript | www.dovepress.com
Dovepress
http://dx.doi.org/10.2147/OTT.S86515

Methods for determining DNA content and, ultimately, ploidy in MM include conventional cytogenetics, fluorescence in situ hybridization (FISH), comparative genomic hybridization, and, recently, massively parallel whole genome sequencing. Because unique mutations have been observed in individual human cancer samples, the identification and characterization of the molecular alterations of individual cancer patients is a critical step toward the development of more effective personalized therapies. For example, next-generation sequencing (NGS) technologies have revolutionized cancer genomics research by providing a comprehensive method of detecting genomic alterations associated with somatic cancer.[7–9] In this study, we sequenced all exons of 409 cancer-related genes in matched tumor and normal DNA samples from a multidrug-resistant myeloma patient using a next-generation semiconductor sequencing protocol.

Case report

A 69-year-old male presented in October 2010 with back pain. Physical examination and magnetic resonance imaging revealed large focal lesions in the fourth thoracic vertebra (Figure 1A) and first lumbar vertebra (Figure 1B). Laboratory evaluation revealed a white blood cell count of 2.5×10^3/μL with no atypical cells, a red blood cell count of 3.67×10^6/μL, a hemoglobin level of 11.6 g/dL, and a platelet count of 122×10^6/μL. The serum total protein level was 10.7 g/dL, the albumin level was 3.4 g/dL, the serum β2 microglobulin level was 4.2 mg/dL, and the serum calcium level was 8.9 mg/dL. The concentrations of IgG, IgA, and IgM were 6,284, 34, and 25 mg/dL, respectively. The monoclonal protein IgG was increased, and serum immunofixation revealed the production of IgG with λ light-chain restriction (data not shown). The proliferation of plasma cells (more than 10% among all nucleated cells) was also detected in BM aspirates. When BM biopsy was performed, the infiltration of plasma cells expressing IgG λ monoclonal protein was identified by pathological investigation, and the patient was diagnosed with MM (Stage II according to the International Staging System). Chromosome analysis at this time using conventional Giemsa banding of BM-derived metaphase spreads revealed a normal karyotype (46, XX) in all analyzed cells. The patient was then treated with one cycle of high-dose dexamethasone, followed by three cycles of bortezomib plus dexamethasone. He achieved complete response according to the International Myeloma Working Group uniform response criteria. His symptoms were also significantly improved.

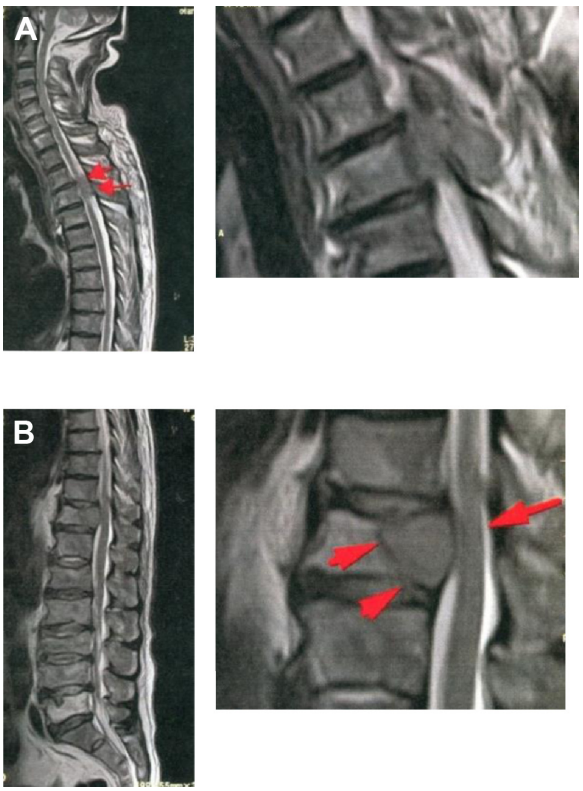

Figure 1 Sagittal T1-weighted magnetic resonance images depict focuses of plasma cell infiltration and pathologic fractures in the T4 (**A**) and L1 (**B**) vertebrae.
Note: Red arrows indicate large focal lesions in the vertebrae.

In August 2012, the serum concentrations of IgG and free light chain (FLC) gradually increased, suggesting the worsening of his MM. His complete blood count was as follows: 1.8×10^3/μL white blood cells, 3.61×10^6/μL red blood cells, 11.6 g/dL hemoglobin, and 55×10^6/μL platelets. BM analysis showed complex aberrations often observed in this patient (Figures 2A and 2B) and an elevated plasma cell percentage (59.8%). His karyotype was 39, XY, del(1)(p22p36), −3, −6, der(8)t(6:8)(p11.1:p23), −10, t(11:14)(q13:q32), −12, add(13)(q22), add(16)(q22), −17, add(18)(p11), −19, −20, +mar [4]/46, XY [20]. The chromosomal translocation t(11:14)(q13:q32), which generates the IgH/CCND1 fusion gene, was also identified in our case by FISH (Figure 2C).

The patient was started on a bortezomib, cyclophosphamide, and dexamethasone regimen. No serious complications occurred during the course of the treatment, and a partial response was observed with a decrease in the serum FLC value. After seven cycles of this regimen, however, his condition progressively deteriorated, with increases in serum lambda immunoglobulin light chain and LDH, a deterioration of renal function, and the appearance of circulating plasma cells in the peripheral blood (up to 5% of the total peripheral leukocyte population). He was admitted for combination chemotherapy with combination chemotherapy with bortezomib,

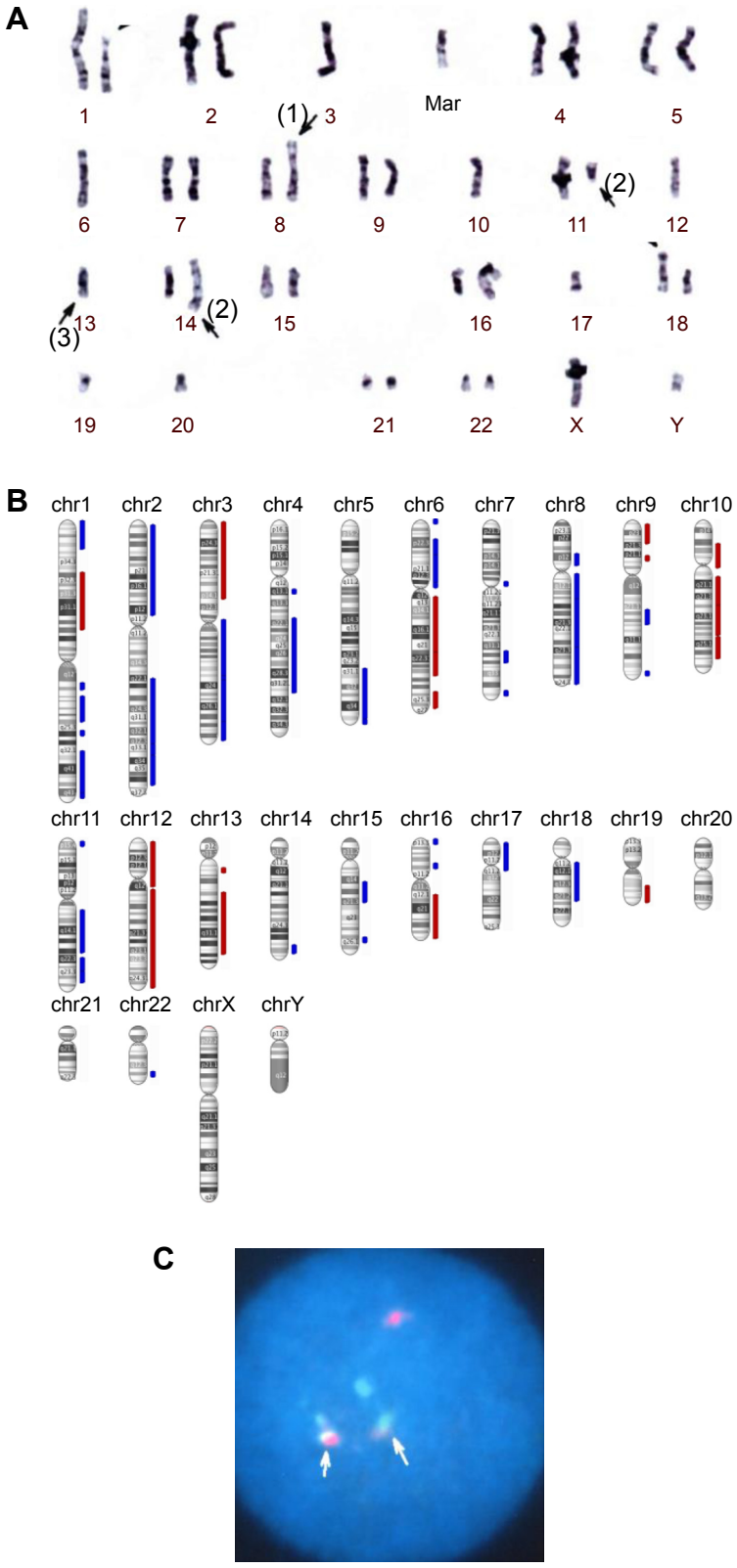

Figure 2 Evaluation of a bone marrow aspirate.

Notes: (**A**) Conventional karyotyping of metaphase cells from BM aspirate was performed using the G-banding technique. Complex cytogenetic aberrancies including loss of chromosomes, and additional uncharacterized materials at chromosome 8 (1) and 13 (2) are shown here. In addition, a dicentric translocation involving chromosome 11 and 14 (3) were also observed. (**B**) Visualization of CNVs over the entire genome in the karyotype view. The decreased copy number is indicated in red with increased copy number indicated in blue. (**C**) Interphase FISH studies were performed on BM aspirates using IgH/CCND1 dual color dual fusion probe (Vysis Inc., Des Plaines, IL, USA). The cell showed one orange (normal CCND1), one green (normal IgH), and two yellow signals (arrows), indicating typical t(11;14) rearrangement.

Abbreviations: CNV, copy number variant; FISH, fluorescence in situ hybridization; BM, bone marrow.

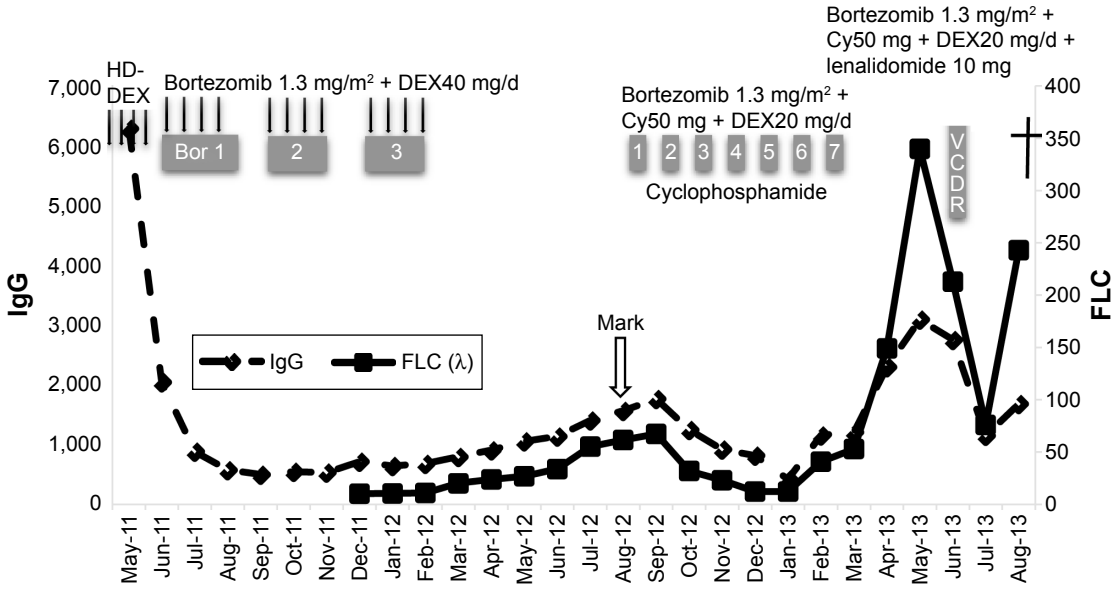

Figure 3 Clinical course of the patient.
Abbreviations: HD, high dose; DEX, dexamethsone; Cy, cyclophosphamide; FLC, free light chain; IgG, Immunoglobulin G.

cyclophosphamide, lenalidomide, and dexamethasone, but his response was poor (Figure 3), and an increase in myeloma cells was detected by BM biopsy. Unfortunately, the patient has since passed away, and his family did not choose to perform postmortem examination.

The patient provided consent for use of his medical record and samples for clinical and research purposes, and the examination was performed in accordance with the Declaration of Helsinki. The sequence study was approved by the Institutional Review Boards of Sapporo Medical University. Retrospectively, to better understand the molecular pathogenesis in this patient, we sequenced 409 cancer-related genes in matched tumor and nontumor DNA samples at relapse in August 2012 using an Ion Torrent PGM (Life Technologies, Carlsbad, CA, USA). DNA was extracted from magnetic bead–enriched BM CD138 positive tumor cells from the patient, and CD138 negative cells were used as matched nontumor cells. DNA (40 ng) was used for multiplex polymerase chain reaction (PCR) amplification with an Ion Ampliseq Comprehensive Cancer Panel (Life Technologies), enabling the targeted coverage of all exons of 409 cancer-related genes frequently cited and mutated (covered regions =95.4% of total). The 15,992 amplicons obtained represented more than 1.2 Mb of target sequence. Library preparation and sequencing with an Ion Torrent PGM was performed as previously described.[9] The mean read depths were 125× (tumor) and 152× (normal). Alignment to the human genome build 19 and variant calling were performed by Ion Reporter Software 4.0. Mutations were also validated by conventional Sanger sequencing. We identified eight nonsynonymous somatic mutations (6.49 mutations/Mb; Table 1). We included missense mutations in seven genes (SYNE1, IKBKB, ERBB3, MYH11, CYLD, TP53, and CDH2) and a frameshift mutation in EGFR. Changes in relative copy number were also assessed from the sequencing data, and we identified 133 copy number variant (CNV) regions, including 87 gain and 46 loss regions (Figure 2B and Table S1). Importantly, we found a gain in the copy number of CCND1, a gene encoding cyclin D1. To check the contamination of tumor cells in the CD138 negative subset, we compared CD138 negative DNA of this patient and peripheral blood DNA from two healthy donors. We found single nucleotide variants in the CD138 negative DNA of this patient; however, all variants had previously been reported in the NCBI dbSNP database (http://www.ncbi.nlm.nih.gov/SNP/) (Tables 2 and 3). Therefore, we can rule out tumor cell contamination in the CD138 negative subset.

Discussion

MM is a plasma cell malignancy characterized by a heterogeneous clinical course. Treatments for MM have remarkably improved in recent years, due in part to the introduction of novel therapies such as bortezomib, thalidomide, and lenalidomide. Despite these advancements, the prognosis of patients with relapse and refractory MM remains poor, and novel therapies are needed. Alternatively, the identification of novel targets or signaling pathways regulating myeloma cell proliferation would improve the clinical outcome and survival of refractory MM patients. Several pathways related to drug resistance and cell survival, such as Notch1, Akt, and NF-κB,

Table 1 Somatic mutations identified in our case

Gene	Function	Exon	Protein	Coding	Total coverage	Variant coverage	Variant frequency (%)
SYNE1	Missense	60	p.Val3187Gly	c.9560T>G	68	11	16.2
EGFR	Frameshift deletion	13	p.Glu513Gly	c.1538_1539delG	235	218	92.8
IKBKB	Missense	9	p.Val241Glu	c.722T>A	125	20	16.0
ERBB3	Missense	25	p.Thr1024Asn	c.3071C>A	158	47	29.7
MYH11	Missense	8	p.Ala275Gly	c.824C>G	70	15	21.4
CYLD	Missense	18	p.Cys791Arg	c.2371T>C	25	15	60.0
TP53	Missense	5	p.Arg158Gly	c.472C>G	79	71	89.9
CDH2	Missense	16	p.Asp906Glu	c.2718C>G	86	16	18.6

Notes: List of total coverage, variant read coverage, and variant frequencies of somatic mutations identified in DNA isolated from BM aspirates of this case. BM mononuclear cells were separated using Ficoll–Paque density sedimentation, and plasma cells were purified by positive selection with anti-CD138 magnetic-activated cell separation microbeads (Miltenyi Biotec, Bergisch Gladbach, Germany). Somatic mutations were detected using statistical approaches in tumor (CD138 positive) and normal (CD138 negative) samples from the Ion Reporter software 4.0 tumor-normal workflow. A sequencing coverage of 25× and a minimum variant frequency of 15% of the total number of distinct tags were used as cutoffs. Mutations were called if they occurred in <1% of reads in the normal control, and were absent from dbSNP and the 1,000 Genomes Project database.
Abbreviation: BM, bone marrow.

Table 2 Nucleotide variants identified in CD138-negative bone marrow aspirates from our case-1

Locus number	Coverage	Variant coverage	Frequency (%)	Gene	Function	Exon	Protein	Coding	dbsnp[a]
chr2:219543924	155	67	43.2	*STK36*	Missense	7	p.Arg240Trp	c.718C>T	rs35038757
chr3:14199887	189	101	53.4	*XPC*	Missense	9	p.Ala499Val	c.1496C>T	rs2228000
chr4:106155185	127	127	100.0	*TET2*	Missense	3	p.Pro29Arg	c.86C>G	rs12498609
chr4:1801064	158	60	38.0	*FGFR3*	Missense	3	p.Gly65Arg	c.193G>A	rs2305178
chr4:1807488	100	48	48.0	*FGFR3*	Missense	13	p.Val555Leu	c.1663G>T	rs199544087
chr4:55139771	328	155	47.3	*PDGFRA*	Missense	10	p.Ser478Pro	c.1432T>C	rs35597368
chr4:55981531	153	59	38.6	*KDR*	Missense	4	p.Val136Met	c.406G>A	rs35636987
chr5:176637576	102	102	100.0	*NSD1*	Missense	5	p.Ser726Pro	c.2176T>C	rs28932178
chr5:256509	134	61	45.5	*SDHA*	Missense	15	p.Val657Ile	c.1969G>A	rs6962
chr5:7878179	139	79	56.8	*MTRR*	Missense	5	p.Ser202Leu	c.605C>T	rs1532268
chr6:152443756	115	60	52.2	*SYNE1*	Missense	146	p.Gly8737Ser	c.26209G>A	rs2295191
chr6:32190390	150	148	98.7	*NOTCH4*	Missense	3	p.Lys117Gln	c.349A>C	rs915894
chr6:56351972	143	74	51.7	*DST*	Missense	81	p.Leu4874Val	c.14620C>G	rs80260070
chr6:56417545	104	103	99.0	*DST*	Missense	55	p.Thr3230Ala	c.9688A>G	rs4715631
chr6:56463410	144	72	50.0	*DST*	Missense	40	p.Gln1812Arg	c.5435A>G	rs4712138
chr7:6026988	140	67	47.9	*PMS2*	Missense	11	p.Pro470Ser	c.1408C>T	rs1805321
chr7:91712698	220	101	45.9	*AKAP9*	Missense	33	p.Asn2792Ser	c.8375A>G	rs6960867
chr8:145741439	180	105	58.3	*RECQL4*	Missense	5	p.Arg355Gln	c.1064G>A	rs374743591
chr10:43610119	230	111	48.3	*RET*	Missense	11	p.Gly691Ser	c.2071G>A	rs1799939
chr10:70332672	226	117	51.8	*TET1*	Missense	2	p.Ser193Thr	c.577T>A	rs12773594
chr12:49431094	189	94	49.7	*KMT2D*	Missense	34	p.Met3349Val	c.10045A>G	rs80149580
chr14:51224417	141	74	52.5	*NIN*	Missense	18	p.Pro1111Ala	c.3331C>G	rs2236316
chr14:92460227	200	98	49.0	*TRIP11*	Missense	15	p.Glu1696Lys	c.5086G>A	rs80200454
chr14:92472416	87	48	55.2	*TRIP11*	Missense	11	p.Ser635Cys	c.1904C>G	rs59635749
chr15:40898643	173	77	44.5	*CASC5*	Missense	4	p.Arg43Thr	c.128G>C	rs7177192
chr15:40913840	208	92	44.2	*CASC5*	Missense	10	p.Ala460Ser	c.1378G>T	rs2412541
chr15:40914177	114	54	47.4	*CASC5*	Missense	10	p.Met572Thr	c.1715T>C	rs11858113
chr15:40915190	148	78	52.7	*CASC5*	Missense	10	p.Arg910Gly	c.2728A>G	rs8040502
chr15:40916632	173	78	45.1	*CASC5*	Missense	10	p.Asp1390Glu	c.4170T>A	rs141726041
chr15:41805237	149	72	48.3	*LTK*	Missense	2	p.Arg42Gln	c.125G>A	rs2305030
chr17:5462805	136	67	49.3	*NLRP1*	Missense	4	p.Arg404Gln	c.1211G>A	rs3744718
chr18:47800179	147	61	41.5	*MBD1*	Missense	12	p.Pro401Ala	c.1201C>G	rs125555
chr18:50832072	125	73	58.4	*DCC*	Missense	13	p.Leu679Arg	c.2036T>G	rs2271042
chr19:18876309	106	52	49.1	*CRTC1*	Missense	10	p.Thr344Ala	c.1030A>G	rs3746266

Notes: DNA was extracted from CD138-negative BM aspirates of this case and peripheral blood of healthy donor-1 (TT) using the QIAamp DNA Mini kit (Qiagen GmbH, Hilden, Germany) following manufacturer's instructions. DNA (40 ng) was used for multiplex PCR amplification with an Ion Ampliseq Comprehensive Cancer Panel (Life Technologies, Carlsbad, CA,USA), enabling the targeted coverage of all exons of 409 cancer-related genes in a 4-tube reaction (covered regions =95.4% of total). Nucleotide variants on the CD138-negative BM aspirates of this case were detected using the peripheral blood of healthy donor-1 as a normal control. A sequencing coverage of 25× and a minimum variant frequency of 15% of the total number of distinct tags were used as cutoffs. [a]dbSNP ID number.
Abbreviations: BM, bone marrow; PCR, polymerase chain reaction.

Table 3 Nucleotide variants identified in CD138 negative bone marrow aspirates from our case-2

Locus number	Coverage	Variant coverage	Frequency (%)	Gene	Codon	Exon	Protein	Coding	dbsnp[a]
chr1:114948281	64	63	98.4	*TRIM33*	Missense	15	p.Ile840Thr	c.2519T>C	rs6537825
chr1:144879485	120	28	23.3	*PDE4DIP*	Missense	27	p.Thr1322Arg	c.3965C>G	rs113467089
chr1:206665052	136	68	50.0	*IKBKE*	Missense	18	p.Ala602Val	c.1805C>T	rs12059562
chr1:226555302	223	119	53.4	*PARP1*	Missense	17	p.Val762Ala	c.2285T>C	rs1136410
chr2:219543924	155	67	43.2	*STK36*	Missense	7	p.Arg240Trp	c.718C>T	rs35038757
chr4:1801064	158	60	38.0	*FGFR3*	Missense	3	p.Gly65Arg	c.193G>A	rs2305178
chr4:1807488	100	48	48.0	*FGFR3*	Missense	13	p.Val555Leu	c.1663G>T	rs199544087
chr4:55139771	328	155	47.3	*PDGFRA*	Missense	10	p.Ser478Pro	c.1432T>C	rs35597368
chr4:55981531	153	59	38.6	*KDR*	Missense	4	p.Val136Met	c.406G>A	rs35636987
chr5:256509	134	61	45.5	*SDHA*	Missense	15	p.Val657Ile	c.1969G>A	rs6962
chr5:38496637	214	94	43.9	*LIFR*	Missense	13	p.Asp578Asn	c.1732G>A	rs3729740
chr5:7878179	139	79	56.8	*MTRR*	Missense	5	p.Ser202Leu	c.605C>T	rs1532268
chr6:152443756	115	60	52.2	*SYNE1*	Missense	146	p.Gly8737Ser	c.26209G>A	rs2295191
chr6:51890823	157	87	55.4	*PKHD1*	Missense	32	p.Ala1262Val	c.3785C>T	rs9296669
chr6:51914956	104	52	50.0	*PKHD1*	Missense	22	p.Arg760Cys	c.2278C>T	rs9370096
chr6:56351972	143	74	51.7	*DST*	Missense	81	p.Leu4874Val	c.14620C>G	rs80260070
chr6:56417282	157	157	100.0	*DST*	Missense	55	p.Met3317Ile	c.9951G>A	rs4715630
chr6:56417545	104	103	99.0	*DST*	Missense	55	p.Thr3230Ala	c.9688A>G	rs4715631
chr7:106509331	138	63	45.7	*PIK3CG*	Missense	2	p.Ser442Tyr	c.1325C>A	rs17847825
chr8:145741439	180	105	58.3	*RECQL4*	Missense	5	p.Arg355Gln	c.1064G>A	rs374743591
chr9:8518052	124	67	54.0	*PTPRD*	Missense	21	p.Gln447Glu	c.1339C>G	rs10977171
chr10:43610119	230	111	48.3	*RET*	Missense	11	p.Gly691Ser	c.2071G>A	rs1799939
chr12:49431094	189	94	49.7	*KMT2D*	Missense	34	p.Met3349Val	c.10045A>G	rs80149580
chr14:51202311	140	69	49.3	*NIN*	Missense	28	p.Gln1934Glu	c.5800C>G	rs2295847
chr14:92460227	200	98	49.0	*TRIP11*	Missense	15	p.Glu1696Lys	c.5086G>A	rs80200454
chr14:92472416	87	48	55.2	*TRIP11*	Missense	11	p.Ser635Cys	c.1904C>G	rs59635749
chr15:39880822	330	157	47.6	*THBS1*	Missense	10	p.Thr523Ala	c.1567A>G	rs2292305
chr15:40914177	114	54	47.4	*CASC5*	Missense	10	p.Met572Thr	c.1715T>C	rs11858113
chr15:40916632	173	78	45.1	*CASC5*	Missense	10	p.Asp1390Glu	c.4170T>A	rs141726041
chr15:41805237	149	72	48.3	*LTK*	Missense	2	p.Arg42Gln	c.125G>A	rs2305030
chr16:15820863	305	305	100.0	*MYH11*	Missense	29	p.Ala1241Thr	c.3721G>A	rs16967494
chr18:47800179	147	61	41.5	*MBD1*	Missense	12	p.Pro401Ala	c.1201C>G	rs125555
chr18:50832072	125	73	58.4	*DCC*	Missense	13	p.Leu679Arg	c.2036T>G	rs2271042
chr22:42526694	112	76	67.9	*CYP2D6*	Missense	1	p.Pro34Ser	c.100C>T	rs1065852

Notes: DNA was extracted from CD138 negative BM aspirates of this case and peripheral blood of healthy donor 2 (Y.S.) using the QIAamp DNA Mini kit (Qiagen GmbH, Hilden, Germany) following manufacturer's instructions. DNA (40 ng) was used for multiplex PCR amplification with an Ion Ampliseq Comprehensive Cancer Panel (Life Technologies, Carlsbad, CA, USA), enabling the targeted coverage of all exons of 409 cancer-related genes in a four tube reaction (covered regions =95.4% of total). Nucleotide variants on the CD138-negative BM aspirates of this case were detected using the peripheral blood of healthy donor-2 as a normal control. A sequencing coverage of 25× and a minimum variant frequency of 15% of the total number of distinct tags were used as cutoffs. [a]dbSNP ID number.
Abbreviations: BM, bone marrow; PCR, polymerase chain reaction.

are activated to protect MM cells from death.[10–12] Here, we describe the characterization of genetic abnormalities found in myeloma cells in a patient with refractory MM.

In nonhyperdiploid MM, the IgH gene (14q32) commonly fuses with FGFR3 (4p16), MMSET (4p16.3), CCND3 (6p21), CCND1 (11q13), and MAF (16q23), resulting in the direct or indirect dysregulation of cyclin D.[13] Among the nonhyperdiploid myelomas, the hypodiploid subtype (≦44 chromosomes) has the most aggressive clinical phenotype, but the genetic differences between the groups have not been completely defined. Cytogenetic analysis revealed that this patient had a hypodiploid karyotype with 39 chromosomes and complex chromosomal abnormalities, including t(11:14)(q13:q32). CCND1 expression is generally related to copy number aberrations. Although we did not analyze CCND1 mRNA expression, CNV analysis revealed a gain of 11q13–q21, suggesting the presence of cyclin D1 dysregulation.

Several NGS platforms are available for the sequencing of targeted genomic regions to analyze a variety of disease-associated changes, such as point mutations, insertions, deletions, and CNVs. CNV analysis of the sequencing data revealed that this patient had diverse DNA copy number

alterations, including large and regional gains and losses (Figure 2B and Table S1). Additionally, we detected eight somatic mutations among 409 cancer-related genes (Table 1). We considered gene sets based on existing insights into the biology of this MM patient. It has been proposed that activation of the NF-kB pathway is important in the pathogenesis of MM, as well as in resistance to chemotherapy. We observed two point mutations and three CNVs affecting NF-κB pathway genes, including IKBKB, CYLD, IKBKE, CD79B, and SYK (Tables 1 and S1). Although additional experiments are required to establish the functional significance of genetic alterations of these genes in MM cells, NF-κB pathway activation may be involved in the molecular pathogenesis of this patient's disease.

Alterations in the tumor suppressor retinoblastoma (RB) and p53 or their respective pathways are frequently observed in human cancers.[14] In MM, a deletion or mutation of p53 (17p13) or RB1 (13q14.2) is considered to be predictive of poor prognosis. We found a monoallelic chromosome 17 deletion and a missense mutation in the DNA-binding domain of p53 (Arg158Gly), suggesting the abrogation of p53 transcription. Moreover, the deletion of the CNV in 13q14.2 was detected in this patient, resulting in the inactivation of two key regulators of the cell cycle, RB1 and p53.

A recent study has described an increased rate of mutations in receptor tyrosine kinases (RTKs) and their associated signaling effectors, pointing to a more potent role of this pathway in MM than was previously appreciated.[15] We found two mutations in RTKs, including a missense mutation in ERBB3 and a truncating mutation in EGFR, and have suggested a role of aberrant RTK signaling in the development or progression of MM in this patient. In addition, few studies have addressed the functional roles of the remaining three mutated genes (SYNE1, MYH11, and CDH2) in myeloma, and further investigations are required. SYNE1 is frequently silenced by DNA methylation in primary cancers of the colon and lung,[16,17] suggesting that a loss of SYNE1 function may be a genetic event that promotes tumor progression. MYH11 is a member of the myosin family, and inversion at the MYH11 locus is found in acute myeloid leukemia.[18] Additionally, MYH11 mutations have been shown to occur in human colorectal cancers with microsatellite instability.[19] N-cadherin, encoded by the CDH2 gene, is a transmembrane protein and plays an important role in cell adhesion. Recently, circulating N-cadherin levels was reported to be a negative prognostic factor in patients with MM.[20] In this study, we performed comprehensive genomic analyses using PCR target enrichment and semiconductor-based sequencing of matched tumor and normal DNA samples obtained from an individual with refractory MM. We detected several genetic alterations that may have been associated with the poor prognosis and poor response to chemotherapy of this patient. Although its value should be further confirmed in larger samples, targeted NGS is considered a valuable tool for high-throughput genetic testing in clinical research.

Acknowledgments

This work was supported in part by the Scientific Support Programs for Cancer Research Grant-in-Aid Scientific Research on Innovative Areas Ministry of Education, Culture, Sports, Science, and Technology. This is the same research abstract number 4424 AACR Annual Meeting Philadelphia 2015.

Disclosure

The authors report no conflicts of interest in this work.

References

1. Ikeda H, Hideshima T, Fulciniti M, et al. The monoclonal antibody nBT062 conjugated to cytotoxic Maytansinoids has selective cytotoxicity against CD138-positive multiple myeloma cells in vitro and in vivo. *Clin Cancer Res*. 2009;15:4028–4037.
2. Görgün G, Calabrese E, Hideshima T, et al. A novel Aurora-A kinase inhibitor MLN8237 induces cytotoxicity and cell-cycle arrest in multiple myeloma. *Blood*. 2010;115:5202–5213.
3. Anderson KC. Therapeutic advances in relapsed or refractory multiple myeloma. *J Natl Compr Canc Netw*. 2013;11:676–679.
4. Röllig C, Knop S, Bornhäuser M. Multiple myeloma. *Lancet*. 2015; 385(9983):2197–2208.
5. Chinen Y. Phosphoinositide protein kinase PDPK1 is a crucial cell signaling mediator in multiple myeloma. *Cancer Res*. 2014;74:7418–7429.
6. Görgün G, Calabrese E, Soydan E, et al. Immunomodulatory effects of lenalidomide and pomalidomide on interaction of tumor and bone marrow accessory cells in multiple myeloma. *Blood*. 2010;116: 3227–3237.
7. Damerla RR, Chatterjee B, Li Y, Francis RJ, Fatakia SN, Lo CW. Ion Torrent sequencing for conducting genome-wide scans for mutation mapping analysis. *Mamm Genome*. 2014;3–4:120–128.
8. Singh RR, Patel KP, Routbort MJ, et al. Clinical validation of a next-generation sequencing screen for mutational hotspots in 46 cancer-related genes. *J Mol Diagn*. 2013;5:607–622.
9. Chapman MA. Initial genome sequencing and analysis of multiple myeloma. *Nature*. 2011;471:467–472.
10. Nefedova Y, Cheng P, Alsina M, et al. Involvement of Notch-1 signaling in bone marrow stroma-mediated de novo drug resistance of myeloma and other malignant lymphoid cell lines. *Blood*. 2004;103: 3503–3510.
11. Hideshima T, Catley L, Raje N, et al. Inhibition of Akt induces significant downregulation of survivin and cytotoxicity in human multiple myeloma cells. *Br J Haematol*. 2007;138:783–791.
12. Markovina S, Callander NS. Bortezomib-resistant nuclear factor-kappa B activity in multiple myeloma cells. *Mol Cancer Res*. 2008;6: 1356–1364.
13. Jimenez-Zepeda VH, Braggio E, Fonseca R, et al. Dissecting karyotypic patterns in non-hyperdiploid multiple myeloma: an overview on the karyotypic evolution. *Clin Lymphoma Myeloma Leuk*. 2013;13: 552–558.

14. Fonseca R, Blood E, Rue M, Harrington D, et al. Clinical and biologic implications of recurrent genomic aberrations in myeloma. *Blood*. 2003; 101:4569–4575.
15. Leich E, Weißbach S, Klein HU, et al. Multiple myeloma is affected by multiple and heterogeneous somatic mutations in adhesion- and receptor tyrosine kinase signaling molecules. *Blood Cancer J*. 2013;3:102.
16. Tessema M, Willink R, Do K, et al. Promoter methylation of genes in and around the candidate lung cancer susceptibility locus 6q23–25. *Cancer Res*. 2008;68:1707–1714.
17. Schuebel KE, Chen W, Cope L, Glöckner SC, et al. Comparing the DNA hypermethylome with gene mutations in human colorectal cancer. *PLoS Genet*. 2007;3(9):1709–1723.
18. Castilla LH, Garrett L, Adya N, et al. The fusion gene Cbfb-MYH11 blocks myeloid differentiation and predisposes mice to acute myelomonocytic leukaemia. *Nat Genet*. 1999;23(2):144–146.
19. Alhopuro P, Phichith D, Tuupanen S, et al. Unregulated smooth-muscle myosin in human intestinal neoplasia. *Proc Natl Acad Sci U S A*. 2008; 105(14):5513–5518.
20. Vandyke K, Chow AW, Williams SA, et al. Circulating N-cadherin levels are a negative prognostic indicator in patients with multiple myeloma. *Br J Haematol*. 2013;161(4):499–507.

Supplementary material

Table S1

Locus	Ploidy	Length (bp)	Gene
1p36.31(6531783–6532696)	9	913	PLEKHG5
1p36.31(6534071–6534252)	9	181	PLEKHG5
1p36.22(11204731–11317231)	3	112,500	MTOR:MTOR–AS1
1p33(47685376–47838806)	4	153,430	TAL1:CMPK1
1p33p13.2(47840544–114940663)	1	67,100,119	CMPK1:CDKN2C:JUN:JAK1:BCL10:LOC646626:DPYD:DPYD–AS1:TRIM33
1p13.2p12(115006125–120491804)	1	5,485,679	TRIM33:NRAS:NOTCH2
1q21.1(144882848–144922543)	3	39,695	PDE4DIP
1q21.1(144922543–144946743)	1	24,200	PDE4DIP
1q25.3q31.1(185069308–186287597)	1	1,218,289	RNF2:MIR548F1:PRG4:TPR
1q31.1(186287597–186315401)	3	27,804	MIR548F1:TPR
1q31.1(186340019–186645716)	6	305,697	MIR548F1:TPR:PTGS2
1q32.1(204396791–204438963)	3	42,172	PIK3C2B
1q32.1(204494558–204518660)	1	24,102	MDM4
1q32.1(204518660–206652476)	4	2,133,816	MDM4:IKBKE
1q43(237037987–237060883)	5	22,896	MTR
1q44(243776889–243809266)	0	32,377	AKT3
2p25.2(5832763–5833155)	10	392	SOX11
2p25.2p23.3(5833155–24951356)	3	19,118,201	SOX11:MYCN:NCOA1
2p23.3(24952332–24952686)	0	354	NCOA1
2p23.3(24962207–25462090)	4	499,883	NCOA1:DNMT3A
2p21(42509881–47672730)	3	5,162,849	EML4:MSH2
2p21(47672761–47693939)	0	21,178	MSH2
2p21(47698056–47705686)	5	7,630	MSH2
2p16.1p15(61145266–61715462)	1	570,196	REL:XPO1
2q22.1q22.2(141031958–142888394)	3	1,856,436	LRP1B
2q22.3(148657078–148657416)	6	338	ACVR2A
2q31.2q32.2(178096331–190719874)	4	12,623,543	NFE2L2:PMS1
2q33.1(198263157–198266593)	1	3,436	SF3B1
2q33.1(198266665–198274567)	5	7,902	SF3B1
2q33.1q34(198285075–209101941)	4	10,816,866	SF3B1:CREB1:IDH1
2q35q36.1(216288165–223066804)	3	6,778,639	FN1:STK36:PAX3
3p26.2p25.2(3192502–12458385)	1	9,265,883	CRBN:FANCD2:C3orf24:VHL:PPARG RAF1:XPC:TGFBR2:MLH1:ITGA9:MYD88:CTNNB1:LTF:SETD2:BAP1: PBRM1:M
3p25.2p13(12641643–70014401)	1	57,372,758	AGI1:MITF
3p13(71008300–71015133)	0	6,833	FOXP1
3p13(71015133–71247590)	1	232,457	FOXP1
3q22.3q23(138425984–142178221)	4	3,752,237	PIK3CB:FOXL2:ATR
3q23(142180753–142185454)	10	4,701	ATR
3q23(142186790–142226819)	4	40,029	ATR
3q23(142279172–142285045)	4	5,873	ATR
3q26.32q27.3(178916622–187442712)	3	8,526,090	PIK3CA:SOX2–OT:SOX2:LOC100131635:BCL6
3q29(195590930–195622288)	3	31,358	TNK2
4p16.3(1800963–1809006)	3	8,043	FGFR3
4q12q13.1(55987269–62801812)	4	6,814,543	KDR:LPHN3
4q13.1(62863973–62935895)	10	71,922	LPHN3
5q11.2(55259956–55272179)	1	12,223	IL6ST
5q13.1(67522495–67589174)	4	66,679	PIK3R1
5q13.1q22.2(67589211–112111335)	1	44,522,124	PIK3R1:APC
5q22.2(112111335–112176325)	3	64,990	APC
5q31.1q32(131972888–149514586)	3	17,541,698	RAD50:CTNNA1:CSF1R:PDGFRB
5q35.3(176683949–180058790)	3	3,374,841	NSD1:FLT4
6p25.3p22.3(393089–18264237)	5	17,871,148	IRF4:DEK
6p21.32p21.1(32169809–44219786)	4	12,049,977	NOTCH4:DAXX:PIM1:FOXP4:MIR4641:HSP90AB1
6p21.1p12.3(44219786–51720789)	3	7,501,003	HSP90AB1:PKHD1
6p12.3(51720789–51732717)	0	11,928	PKHD1

(*Continued*)

Table S1 (*Continued*)

Locus	Ploidy	Length (bp)	Gene
6p12.3(51732717–51774287)	5	41,570	PKHD1
6p12.2(51882320–51909967)	4	27,647	PKHD1
6p12.2p12.1(52880891–52906053)	7	25,162	ICK
6p12.1(56371186–56373367)	10	2,181	RNU6–71:DST
6p12.1(56373367–56418558)	3	45,191	RNU6–71:DST
6p12.1(56420267–56479190)	4	58,923	RNU6–71:DST
6p12.1(56489295–56505172)	7	15,877	RNU6–71:DST
6q12q252(69348493–152749529)	1	83,401,036	BAI3:MAP3K7:EPHA7:PRDM1:FOXO3:ROS1:SGK1:MYB:TNFAIP3:ESR1:SYNE1
6q25.2(152755037–152762469)	0	7,432	SYNE1
6q25.2q27(152763208–167275671)	1	14,512,463	SYNE1:IGF2R:RPS6KA2
7p22.1(6038830–6048682)	6	9,852	PMS2
7p21.2p112(13978822–55211092)	1	41,232,270	ETV1:IKZF1:EGFR
7p11.2q212(55211092–91632356)	3	36,421,264	EGFR:LOC100507500:SBDS:AKAP9
7q22.1(98478735–98491481)	1	12,746	TRRAP
7q22.1(98491496–98503897)	4	12,401	TRRAP
7q31.2(116398533–116409750)	1	11,217	MET
7q31.2q31.33(116409750–126882846)	3	10,473,096	MET:POT1:GRM8
7q36.1(151873440–151884429)	3	10,989	MLL3
7q36.1(151884429–151896501)	6	12,072	MLL3
8p12(30915961–31015061)	1	99,100	WRN
8p11.21(41801269–41838483)	4	37,214	KAT6A
8q11.21(48761708–48842433)	3	80,725	PRKDC
8q11.21(48848199–48848467)	9	268	PRKDC
8q13.3(71056866–71068855)	4	11,989	NCOA2
8q22.3(103271231–103284984)	4	13,753	UBR5
8q22.3(103287769–103288057)	0	288	UBR5
8q22.3q23.3(103301703–113267690)	3	9,965,987	UBR5:CSMD3
8q23.3(113275800–113326867)	5	51,067	CSMD3
8q23.3(113353734–113697671)	4	343,937	CSMD3
9p24.1(5021975–5055745)	1	33,770	JAK2
9p24.1(5069115–5080629)	0	11,514	JAK2
9p24.1p13.2(5080644–37034041)	1	31,953,397	JAK2:PTPRD:PSIP1:CDKN2A:CDKN2B–AS1:CDKN2B:TAF1L:FANCG:PAX5
9q21.2q22.2(80336237–93607934)	3	13,271,697	GNAQ SYK
10p12.31(21971114–22019887)	4	48,773	MLLT10
10p12.31q24.32(22030804–104155714)	1	82,124,910	MLLT10:RET:MAPK8:NCOA4:TET1:KAT6B:BMPR1A:PTEN:ACTA2:FAS:CYP2C19:BLNK:TLX1
1 0q24.32q26.13(104157967–123353360)	1	19,195,393	NFKB2:SUFU:TCF7L2:FGFR2
11p15.5p15.4(532629–3714618)	3	3,181,989	HRAS:INS–IGF2:IGF2:NUP98
11p15.4(3794886–4144704)	1	349,818	NUP98:RRM1
11p15.4(4147854–4159656)	4	11,802	RRM1
11q13.1q21(64577195–95712842)	3	31,135,647	MEN1:CCND1:NUMA1:MRE11A:MAML2
11q21(95826628–96075072)	6	248,444	MAML2:MIR1260B
11q22.2(102195186–102221298)	3	26,112	BIRC3:BIRC2
11q22.3(108126821–108202634)	3	75,813	ATM
11q22.3(108202640–108205758)	8	3,118	ATM
12p13.32q12(4383139–43825146)	1	39,442,007	CCND2:ING4:ZNF384:KRAS:ADAMTS20
12q12q24.33(43845982–132562299)	1	88,716,317	ADAMTS20:ARID2:MLL2:ATF1:SMUG1:ERBB3:DDIT3:CDK4:MDM2:PTPN11:HNF1A:HCAR1:EP400
13q12.13q14.2(26828777–48881526)	1	22,052,749	CDK8:FLT3:FLT1:FOXO1:RB1
13q14.2(48916694–48955639)	0	38,945	RB1
13q14.2q34(49027105–113976789)	1	64,949,684	RB1:BIVM–ERCC5:ERCC5:IRS2:LAMP1
14q32.12(92435944–92470292)	1	34,348	TRIP11
14q32.2q32.31(99697796–102549592)	4	2,851,796	BCL11B:HSP90AA1
14q32.31q32.33(102568334–105259056)	4	2,690,722	HSP90AA1:AKT1
15q14q15.1(39881158–40914530)	3	1,033,372	THBS1:BUB1B:PAK6:CASC5

(*Continued*)

Table S1 (*Continued*)

Locus	Ploidy	Length (bp)	Gene
15q15.1(40914530–40914946)	8	416	CASC5
15q15.1q21.3(40915027–57574785)	3	16,659,758	CASC5:LTK:TGM7:TCF12
15q26.1(91293154–91304549)	4	11,395	BLM
15q26.1(91306116–91358510)	1	52,394	BLM
16p13.3(2110598–2110873)	7	275	TSC2
16p13.3(2126481–2129066)	8	2,585	TSC2
16p13.3(2129066–3824694)	3	1,695,628	TSC2:CREBBP
16p12.2(23614957–23646619)	1	31,662	PALB2
16p12.2p12.1(23646619–27460675)	3	3,814,056	PALB2:IL21R:LOC283888
16q12.1(50825401–50827575)	0	2,174	CYLD
16q12.1q24.3(50828113–89882998)	1	39,054,885	CYLD:MMP2:CDH1:CDH5:CDH1:MAF:ZNF276:FANCA
17p13.2(5405081–5442941)	4	37,860	NLRP1
17p13.1(8046119–8053735)	5	7,616	PER1
17p13.1(8108179–8111176)	4	2,997	AURKB
17p12q11.2(12016465–29663487)	3	17,647,022	MAP2K4:FLCN:NF1
17q11.2(29663487–29663721)	0	234	NF1
17q11.2(29663721–29684308)	4	20,587	NF1
17q23.3q25.3(62008693–75398324)	4	13,389,631	CD79B:PRKAR1A:SEPT9
17q25.3(78346858–78363051)	3	16,193	RNF213:LOC100294362
19q13.2(42788861–42799411)	0	10,550	CIC
19q13.32q13.43(45252220–57746806)	1	12,494,586	BCL3:MARK4:ERCC2:CD3EAP:ERCC1:PPP2R1A:AURKC
20q12(39708708–40730948)	3	1,022,240	TOP1:PLCG1:PTPRT
21q22.2q22.3(39947501–46330714)	3	6,383,213	ERG:ITGB2
22q11.21(22127160–22153507)	1	26,347	MAPK1
22q11.23(23523722–23524530)	1	808	BCR
22q13.2(41574270–42526792)	4	952,522	EP300:CYP2D6